The Hybrid High Order method in non-linear solid mechanics with `MFront` and `MGIS`

DE LA RECHERCHE À L'INDUSTRIE

MFront User Day

18/10/2021

D. Siedel, T.Helfer, O.Fandeur, N.Pignet, J.Besson

Table of Contents

Principle of the HHO method

The principle of the HHO method

The HHO method (Di Pietro, Ern, 2015; Pignet, 2018)

- **Displacement jumps** between elements $\rightarrow$ enriched kinematics $\rightarrow$ robustness to volumetric locking
- **Cells** communicate through **faces** under the action of a **traction force**

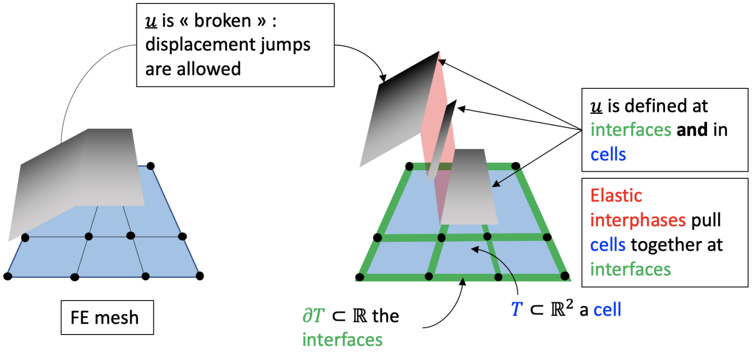

Advantages of the HHO method

- Robust to volumetric locking in **primal formulation**
- Arbitrary polynomial order
- Native support of polyhedral meshes with possibly non-conformal interfaces

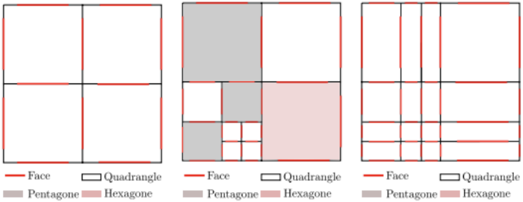

Figure – Example of application of the polyhedral support feature of the HHO method to mesh refinement (Pignet, 2019)

- Attractive numerical costs $\rightarrow$ elimination of cell unknowns

The mechanical setting

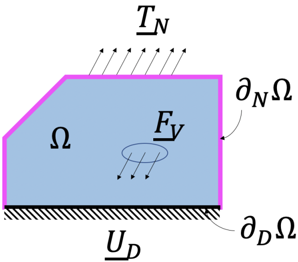

Principle of Virtual Works (PVW)

For all $\underline{\hat{\boldsymbol{u}}}$ kinematically admissible (*i.e.* $\underline{\hat{\boldsymbol{u}}}|_{\partial\Omega} = 0$), $\underline{\boldsymbol{u}}$ verifies :

$$\begin{aligned} \int_\Omega \underset{\sim}{\boldsymbol{PK}}(\nabla_X \underline{\boldsymbol{u}}) : \nabla_X \underline{\hat{\boldsymbol{u}}} &= \int_{\partial_N\Omega} \underline{\boldsymbol{T}}_N \cdot \underline{\hat{\boldsymbol{u}}} + \int_\Omega \underline{\boldsymbol{F}}_V \cdot \underline{\hat{\boldsymbol{u}}} \quad \text{in } \Omega \\ \underline{\boldsymbol{u}} &= \underline{\boldsymbol{U}}_D \quad \text{on } \partial_D\Omega \end{aligned} \tag{1}$$

Constitution of the HHO element

- Let an element **with planar faces** made of the following layers :

Layer	Displacement
cell T	$\underline{\boldsymbol{u}}_T$
boundary ∂T	$\underline{\boldsymbol{u}}_{\partial T}$
interphase Υ	$\underline{\boldsymbol{u}}_\Upsilon$ linear with $[\![\underline{\boldsymbol{u}}]\!] = \underline{\boldsymbol{u}}_T - \underline{\boldsymbol{u}}_{\partial T}$

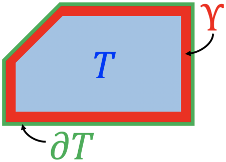

Discontinuity of the displacement between a cell and its boundary

- Υ of thickness ℓ envelopps T and bridges $\underline{\boldsymbol{u}}_T$ to $\underline{\boldsymbol{u}}_{\partial T}$ such that :
  - If $\ell > 0$, the displacement is continuous between T and ∂T through Υ
  - If $\ell \rightarrow 0 \implies \Upsilon \rightarrow \partial T$ the displacement is discontinuous across ∂T

Characterization of the interphase

- Let suppose the elastic interphase Υ a small volume with comparison to the cell $\mathcal{T}$, with a linear elastic behavior :

Hypothesis

- **H1** : $0 < \ell \ll h_{\mathcal{T}}$ such that the displacement in Υ is linear and the deformation homogeneous :

$$\nabla_X \underline{\boldsymbol{u}}|_\Upsilon = \frac{[\![\underline{\boldsymbol{u}}]\!]}{\ell} \otimes \underline{\boldsymbol{n}}_{\partial\mathcal{T}} = \underset{\sim}{\varepsilon}|_\Upsilon \tag{2}$$

- **H2** : Υ is made out of a linear elastic material with Young modulus β and a zero Poisson ratio :

$$\underset{\sim}{\boldsymbol{\sigma}}|_\Upsilon = \beta \underset{\sim}{\varepsilon}|_\Upsilon \tag{3}$$

The stabilization term

- Under hypothesis **H1** and **H2**, the internal energy in $T \cup \Upsilon$ writes as :

$$
\begin{aligned}
\int_{T \cup \Upsilon} \underset{\sim}{\boldsymbol{PK}} : \nabla_X \underline{\hat{\boldsymbol{u}}} &= \int_T \underset{\sim}{\boldsymbol{PK}} : \nabla_X \underline{\hat{\boldsymbol{u}}} + \int_\Upsilon \underset{\sim}{\boldsymbol{\sigma}} : \nabla_X \underline{\hat{\boldsymbol{u}}} \\
&= \int_T \underset{\sim}{\boldsymbol{PK}} : \nabla_X \underline{\hat{\boldsymbol{u}}} + \int_\Upsilon \frac{\beta \ell}{h_{\partial T}} \frac{[\![\underline{\boldsymbol{u}}]\!]}{\ell} \otimes \underline{n}_{\partial T} : \frac{[\![\underline{\hat{\boldsymbol{u}}}]\!]}{\ell} \otimes \underline{n}_{\partial T} \\
&= \int_T \underset{\sim}{\boldsymbol{PK}} : \nabla_X \underline{\hat{\boldsymbol{u}}} + \int_{\partial T} \int_\ell \frac{\beta \ell}{h_{\partial T}} \frac{[\![\underline{\boldsymbol{u}}]\!]}{\ell} \cdot \frac{[\![\underline{\hat{\boldsymbol{u}}}]\!]}{\ell} \\
&= \boxed{\int_T \underset{\sim}{\boldsymbol{PK}} : \nabla_X \underline{\hat{\boldsymbol{u}}} + \int_{\partial T} \frac{\beta}{h_{\partial T}} [\![\underline{\boldsymbol{u}}]\!] \cdot [\![\underline{\hat{\boldsymbol{u}}}]\!]}
\end{aligned}
\tag{4}
$$

- The internal energy is the sum of :
  - the contribution in the cell T
  - the traction force in Υ depending on the stifness β $\rightarrow$ **stabilization** term

The reconstructed gradient

- The reconstructed gradient $\underset{\sim}{\boldsymbol{G}}_T$ is the projection of the gradient of the displacement in $T \cup \Upsilon$

$$\begin{aligned}
&\text{(eq grad)} \iff \int_{T\cup\Upsilon} \left(\underset{\sim}{\boldsymbol{G}}_T - \nabla_X \underline{\boldsymbol{u}}\right) : \underset{\sim}{\tau} = 0 \\
&\forall \text{ tensor } \underset{\sim}{\tau} \\
&\iff \int_{T\cup\Upsilon} \underset{\sim}{\boldsymbol{G}}_T : \underset{\sim}{\tau} = \int_T \nabla_X \underline{\boldsymbol{u}}_T : \underset{\sim}{\tau} + \int_\Upsilon \frac{[\![\underline{\boldsymbol{u}}]\!]}{\ell} \otimes \underline{n}_{\partial T} : \underset{\sim}{\tau} \\
&\iff \int_{T\cup\Upsilon} \underset{\sim}{\boldsymbol{G}}_T : \underset{\sim}{\tau} = \int_T \nabla_X \underline{\boldsymbol{u}}_T : \underset{\sim}{\tau} + \int_{\partial T}\int_\ell \frac{[\![\underline{\boldsymbol{u}}]\!]}{\ell} \cdot \underset{\sim}{\tau}\, \underline{n}_{\partial T} \\
&\iff \boxed{\int_{T\cup\Upsilon} \underset{\sim}{\boldsymbol{G}}_T : \underset{\sim}{\tau} = \int_T \nabla_X \underline{\boldsymbol{u}}_T : \underset{\sim}{\tau} + \int_{\partial T} [\![\underline{\boldsymbol{u}}]\!] \cdot \underset{\sim}{\tau}\, \underline{n}_{\partial T}}
\end{aligned} \tag{5}$$

- $\underset{\sim}{\boldsymbol{G}}_T$ depends on both cell and faces displacements $\rightarrow$ richer formulation

- Making now $\ell \to 0$, the discontinuous case is met :
  - Υ fades into ∂T
  - $\underline{\boldsymbol{u}}_{\Upsilon}$ becomes $[\![\underline{\boldsymbol{u}}]\!] = \underline{\boldsymbol{u}}_T|_{\partial T} - \underline{\boldsymbol{u}}_{\partial T}$
- Taking in the internal contribution :
  - The **reconstructed gradient** $\underset{\sim}{\boldsymbol{G}}_T$ (5) in place of $\nabla_X \underline{\boldsymbol{u}}$
  - The **stabilization term** (or **traction force**) (4)
  - The **element unknown** made of the pair $(\underline{\boldsymbol{u}}_T, \underline{\boldsymbol{u}}_{\partial T})$

The PVW in the context of the HHO method

Find $(\underline{\boldsymbol{u}}_T, \underline{\boldsymbol{u}}_{\partial T})$, such that for all $(\underline{\hat{\boldsymbol{u}}}_T, \underline{\hat{\boldsymbol{u}}}_{\partial T})$ kinematically admissible

$$\begin{aligned}
\int_T \underset{\sim}{\boldsymbol{PK}}(\underset{\sim}{\boldsymbol{G}}_T) : \underset{\sim}{\hat{\boldsymbol{G}}}_T + \int_{\partial T} \frac{\beta}{h_{\partial T}} [\![\underline{\boldsymbol{u}}]\!] \cdot [\![\underline{\hat{\boldsymbol{u}}}]\!] &= \int_T \underline{\boldsymbol{F}}_V \cdot \underline{\hat{\boldsymbol{u}}}_T && \text{in } T \\
&\quad + \int_{\partial_N T} \underline{\boldsymbol{T}}_N \cdot \underline{\hat{\boldsymbol{u}}}_{\partial T} && (6) \\
\underline{\boldsymbol{u}}_{\partial T} &= \underline{\boldsymbol{U}}_D && \text{on } \partial_D T
\end{aligned}$$

Discretization space

- Following the Galerkin method, the discretization spaces are respecitively :
  - polynomials of order l in the cell T : $\mathbb{P}^l(T, \mathbb{R}^d)$
  - polynomials of order k in faces ∂T : $\mathbb{P}^k(\partial T, \mathbb{R}^d)$

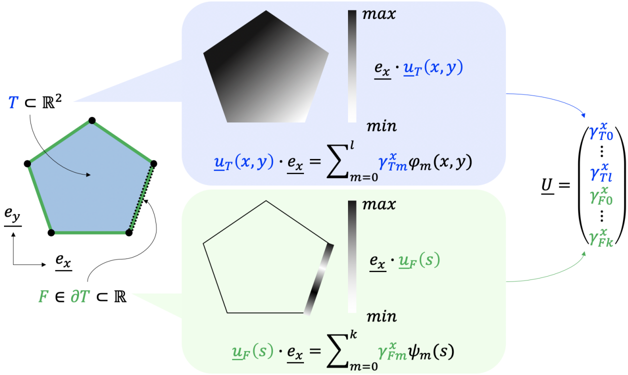

Towards the HHO method

- Presented stabilization term $\rightarrow$ **HDG** (Hybrid Discontinuous Galerkin)
  - Cell polynomial order $l \in [k, k+1]$

Error	$l = k$	$l = k+1$
L^2-norm	h^{k+1}	h^{k+2}
H^1-norm	h^k	h^{k+1}

Table – Convergence rates for the HDG stabilization (Ern, DiPietro, 2015)

- More sophisticated stabilization term $\rightarrow$ **HHO**
  - Cell polynomial order $l \in [k-1, k, k+1]$

Error	$l = k-1$	$l = k$	$l = k+1$
L^2-norm	h^{k+2}	h^{k+2}	h^{k+2}
H^1-norm	h^{k+1}	h^{k+1}	h^{k+1}

Table – Convergence rates for the HHO stabilization (Ern, DiPietro, 2015)

Discretized form

- The equilibrium of the element depends on both cells and faces unknowns :

$$\int_T \underset{\sim}{\boldsymbol{PK}}(\underset{\sim}{\boldsymbol{G}}_T) : \underset{\sim}{\hat{\boldsymbol{G}}}_T + \int_{\partial T} \frac{\beta}{h_{\partial T}} [\![\underline{\boldsymbol{u}}]\!] \cdot [\![\underline{\hat{\boldsymbol{u}}}]\!] = \int_T \underline{\boldsymbol{F}}_V \, \underline{\hat{\boldsymbol{u}}}_T + \int_{\partial_N T} \underline{\boldsymbol{T}}_N \, \underline{\hat{\boldsymbol{u}}}_{\partial T} \tag{7}$$

- Wich gives a system depending on both unknowns in discretized form :

$$\begin{pmatrix} K_{TT} & K_{T\partial T} \\ K_{\partial T T} & K_{\partial T \partial T} \end{pmatrix} \begin{pmatrix} \delta U_T \\ \delta U_{\partial T} \end{pmatrix} = \begin{pmatrix} R_T \\ R_{\partial T} \end{pmatrix} \text{ and } \begin{pmatrix} R_T \\ R_{\partial T} \end{pmatrix} = \begin{pmatrix} F_T^{int} \\ F_{\partial T}^{int} \end{pmatrix} - \begin{pmatrix} F_V \\ T_N \end{pmatrix}$$

- Coupling strategies between cells and faces :
  - Either U_T depends **linearly** on $U_{\partial T}$ $\rightarrow$ **static condensation**
  - Either U_T depends **non-linearly** on $U_{\partial T}$ $\rightarrow$ **cell equilibrium** : the cell is in balance with its faces

Static condensation

- The static condensation algorithm is the one used in the literature (Abbas, Ern, Pignet, 2018)

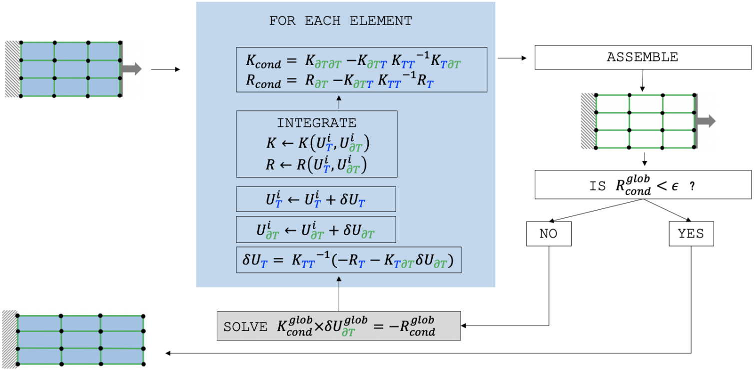

Applications

Notched specimen

- The HHO method is locking free for plane strain computations in finite strain non-linear hardening plasticity

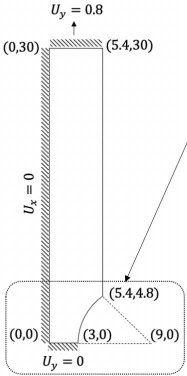

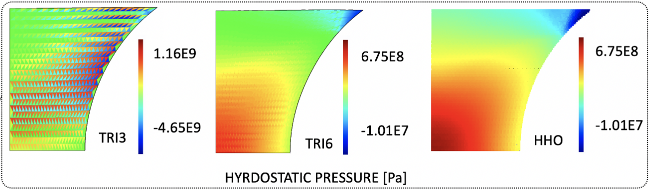

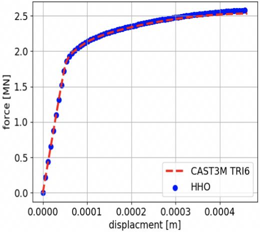

- **Voce hardening plasticity:**

$$\sigma = \sigma_0 + Hp + (\sigma_0 - \sigma_\infty)(1 - e^{-bp})$$

- **Material parameters:**

$E = 206.9$ GPa, $\nu = 0.29$

$H = 129.2$ MPa, $\sigma_0 = 450$ MPa

$\sigma_\infty = 715$ MPa, $b = 16.93$

- The HHO methods is robust to volumetric locking and provides a faster convergence rate than standard FEMs

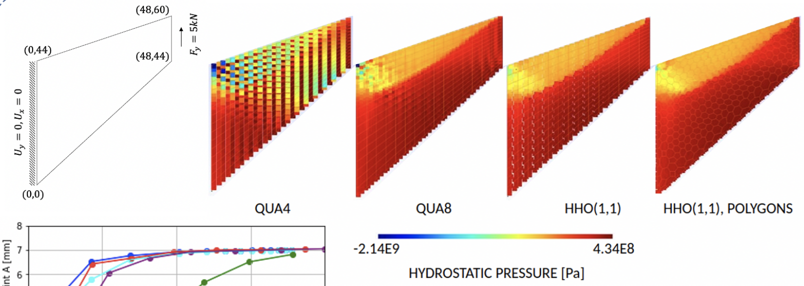

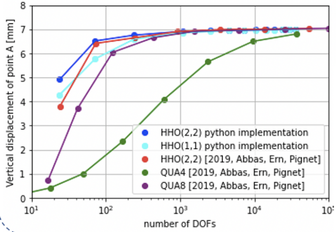

- **Voce hardening plasticity:** $\sigma = \sigma_0 + Hp + (\sigma_0 - \sigma_\infty)(1 - e^{-bp})$
- **Material parameters:**

  $E = 206.9$ GPa, $\nu = 0.29$

  $H = 129.2$ MPa, $\sigma_0 = 450$ MPa, $\sigma_\infty = 715$ MPa, $b = 16.93$

Cook's membrane - Comparison Python/Disk++

- Results are identical for both implementations using the same `MFront` law

- Comparison of the Von Mises stress values for both implementations on an indentical mesh

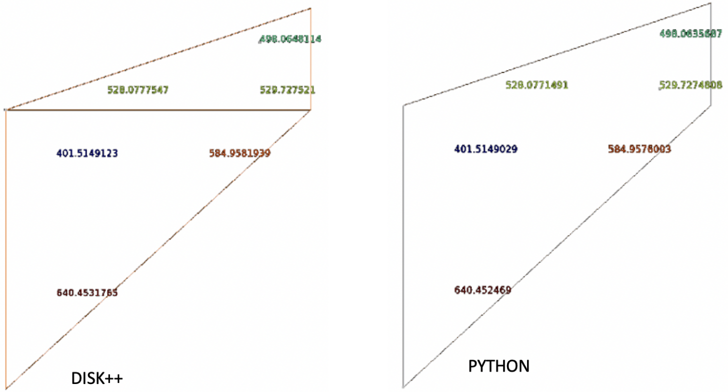

- The trace of the Cauchy stress using the HHO method displays no oscillations, as opposed to the standard finite element one

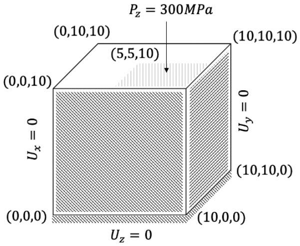

- Perfect plasticity in small deformations:

  $E = 200$ GPa, $\nu = 0.3$, $\sigma_0 = 150$ MPa

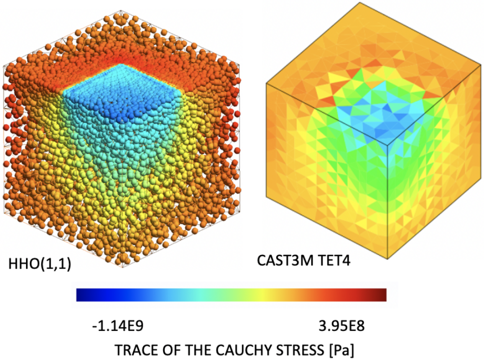

Sphere under internal pressure

- The trace of the Cauchy stress is smooth at the limit load, and in agreement with analytical results

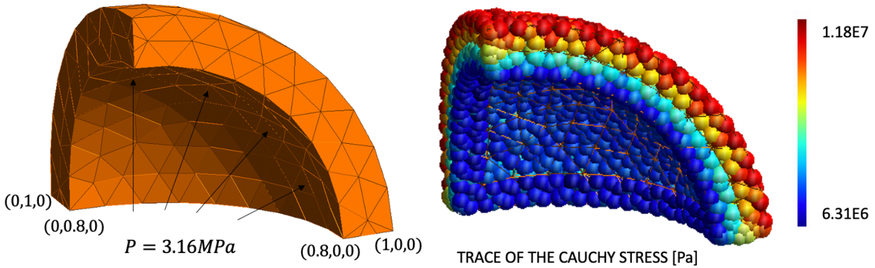

- Perfect plasticity in finite strain: $E = 28.56$ Mpa, $\nu = 0.498$, $\sigma_0 = 6$ Mpa

Pressurized cylinder in axisymmetry

- Linear Elasticity

  $E = 200$ GPa, $\nu = 0.3$

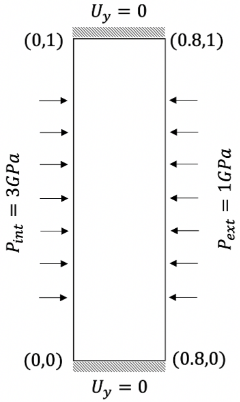

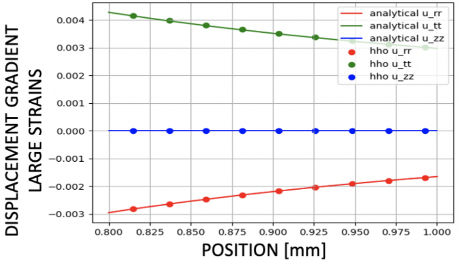

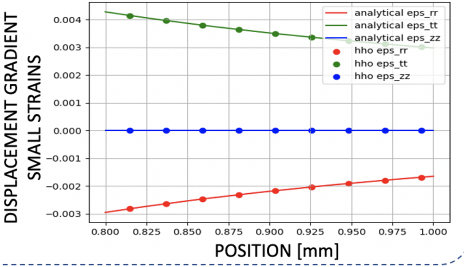

Notched axisymmetric specimen

- Extension of the HHO method to the axisymmetric case

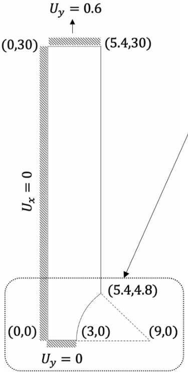

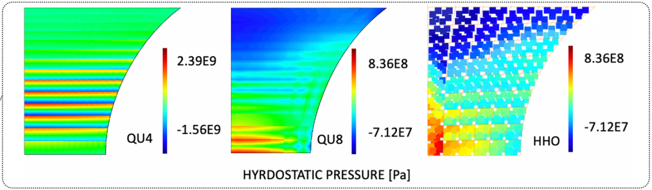

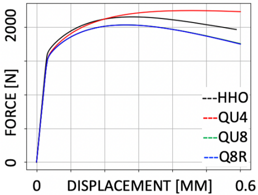

- Voce hardening plasticity:

$$\sigma = \sigma_0 + Hp + (\sigma_0 - \sigma_\infty)(1 - e^{-bp})$$

- Material parameters:

$E = 206.9$ GPa, $\nu = 0.29$
$H = 129.2$ MPa, $\sigma_0 = 450$ MPa
$\sigma_\infty = 715$ MPa, $b = 16.93$

Polyhedral mesh and cristal plasticity

- Using the polyhedral feature of the HHO method for crystal plasticity computations, the Voronoï tesselation is directly exploitable as a mesh

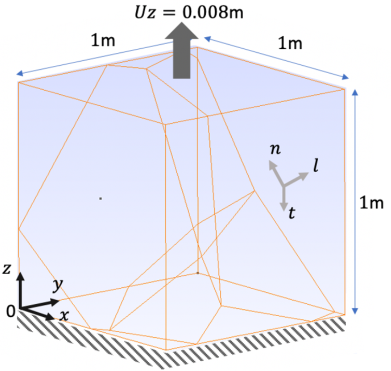

- Meric-Cailletaud Crystal Plasticity in small strains

$$\dot{\gamma}_i = \dot{p}_i \cdot \mathrm{sign}(\tau_i - x_i) \qquad p_i = \int_0^t |\dot{\gamma}_i| dt$$

$$\dot{p}_i = \langle \frac{|\tau_i - x_i| - R_i - \tau_0}{K} \rangle^n \qquad R_i = Q \sum_1^N h_{ij} \cdot (1 - \exp(-b p_j))$$

with $K = 1, n = 10, \tau_0 = 66.62, Q = 11.43, b = 2.1$

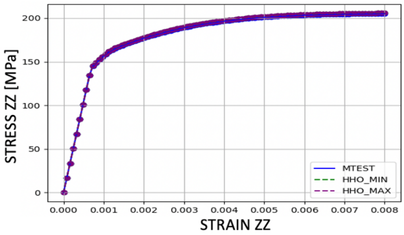

Conclusion and perspectives

Conclusion and perspectives

The HHO method with `MFront + MGIS`

- We recasted the HHO method in a mechanical framework
- `MFront/MGIS` is directly exploitable by an HHO FE code
- It has been tested and validated with `h2o` (python), `Cast3M` and `Disk++`

Perspectives

- Treatment of the irreversibility condition on damage evolution using a local resolution scheme

Figure – Solution to the damage phase field problem on the broken HHO domain